PHYSICAL REVIEW C, VOLUME 65, 061302(R)

Rotational bands with terminating properties in ^{59}Ni

C.-H. Yu,[1] C. Baktash,[1] J. A. Cameron,[2] M. Devlin,[3,*] J. Eberth,[4] A. Galindo-Uribarri,[1] D. S. Haslip,[2,†] D. R. LaFosse,[3,‡] T. J. Lampman,[2] I.-Y. Lee,[5] F. Lerma,[3] A. O. Macchiavelli,[5] S. D. Paul,[1,6] D. C. Radford,[1] I. Ragnarsson,[7] D. Rudolph,[7] D. G. Sarantites,[3] C. E. Svensson,[2,§] J. C. Waddington,[2] J. C. Wells,[8] and J. N. Wilson[2,‖]

[1]*Physics Division, Oak Ridge National Laboratory, Oak Ridge, Tennessee 37831*

[2]*Department of Physics and Astronomy, McMaster University, Hamilton, Ontario, Canada L8S 4M1*

[3]*Chemistry Department, Washington University, St. Louis, Missouri 63130*

[4]*Institut für Kernphysik, Universität zu Köln, D-50937 Köln, Germany*

[5]*Nuclear Science Division, Lawrence Berkeley National Laboratory, Berkeley, California 94720*

[6]*Oak Ridge Institute for Science and Education, Oak Ridge, Tennessee 37831*

[7]*Department of Physics, Lund University, S-22100 Lund, Sweden*

[8]*Department of Physics, Tennessee Technological University, Cookeville, Tennessee 38505*

(Received 4 March 2002; published 31 May 2002)

Highly-deformed rotational bands were established in ^{59}Ni using the ^{40}Ca(^{29}Si,$2p2\alpha$)^{59}Ni reaction. Lifetime measurements indicate that transition quadrupole moments of two of these bands decrease as they smoothly approach their maximum-spin states. The configurations of these bands as well as their band-terminating features are discussed based on configuration-dependent cranked Nilsson-Strutinsky calculations. These calculations indicate that, unlike similar bands observed previously in the region, the two bands in ^{59}Ni maintain significant collectivity at their $I=I_{max}$ states.

DOI: 10.1103/PhysRevC.65.061302 PACS number(s): 21.10.Re, 21.10.Hw, 23.20.Lv, 27.50.+e

Recent experimental studies have established deformed and superdeformed rotational bands in more than ten proton-rich nuclei in the mass $A\sim60$ region. Such systematic experimental data provide a good foundation for the understanding of nuclear collective rotation at large deformation in this mass region, where most nuclei are spherical at low spins and in their ground states. Among these nuclei, two even-even Zn isotopes were found [1,2] to have rotational bands exhibiting typical characteristics of a smooth transition from collective rotation to a noncollective maximal-spin state where all single-particle angular momenta are aligned along the nuclear symmetry axis. Such a transition, or the ''termination'' of collective rotational bands, has also been observed [3,4] in other mass regions. In this Rapid Communication, we report the observation of high-spin rotational bands in the odd-A nucleus ^{59}Ni, which remain partially collective when reaching their $I=I_{max}$ states. Here, I_{max} is defined as the highest spin value allowed by the Pauli principle for a given distribution of valence particles over the open j shells.

With three valence neutrons outside the ^{56}Ni doubly magic core, ^{59}Ni is spherical at low spins and the excited states are best described as single-particle excitations. At higher spins and with added particle hole excitations, collective rotation becomes possible and highly-deformed rotational bands are observed. At even higher angular momentum, these rotational bands exhaust the spin available in their intrinsic configurations, and start approaching noncollective single-particle states again. Such an evolution from highly-deformed collective to single-particle states in a single configuration is indeed a unique laboratory for the study of the interplay between nuclear collective and single-particle motions.

High-spin states in ^{59}Ni were populated using the ^{40}Ca(^{29}Si,$2\alpha2p$) reaction at a beam energy of 130 MeV. The ^{29}Si beam was provided by the 88-Inch Cyclotron at the Lawrence Berkeley National Laboratory, and the target consisted of a layer of 0.5 mg/cm^2 enriched ^{40}Ca evaporated onto a layer of 2.5 mg/cm^2 Ta foil as backing. Prompt-γ rays were detected by the Gammasphere [5] array. The evaporated charged particles were detected by the 95-element CsI detector array Microball [6], and the information obtained was used to select the reaction channel, as well as to determine the velocity of the recoil for event-by-event Doppler corrections. A total of about 39 million two-alpha and two-proton gated $\gamma\gamma\gamma$ or higher-fold events were collected from the experiment.

Four rotational bands were established in ^{59}Ni from the reaction-channel-selected $\gamma\gamma\gamma$ cube, and are shown in Fig. 1 together with a partial level scheme of normally-deformed (ND) low-spin states. All four bands were observed to be in coincidence with the known [7] low-spin transitions in ^{59}Ni. The use of a finite-thickness target backing provided an easy way to differentiate fast- and slow-γ transitions, and quickly led to the identification of deformed bands. The 2.5 mg/cm^2 Ta backing slows down the ^{59}Ni ions from a maximum recoil velocity of $v/c\approx0.040$ to a final velocity (in vacuum) of $v/c\approx0.027$ within 0.3 picoseconds. The fast γ transitions

*Current address: LANSCE-3, MS H855, Los Alamos National Laboratory, Los Alamos, NM 87545.

†Current address: Defense Research Establishment Ottawa, Ottawa, Ontario, Canada K1A 0Z4.

‡Current address: Dept. of Physics, State University of New York at Stony Brook, Stony Brook, NY 11794.

§Current address: Department of Physics, University of Guelph, Guelph, Ontario, Canada N1G 2W1.

‖Current address: Niels Bohr Institute, Blegdamsvej 17, DK-2100 Copenhagen Ø, Denmark.

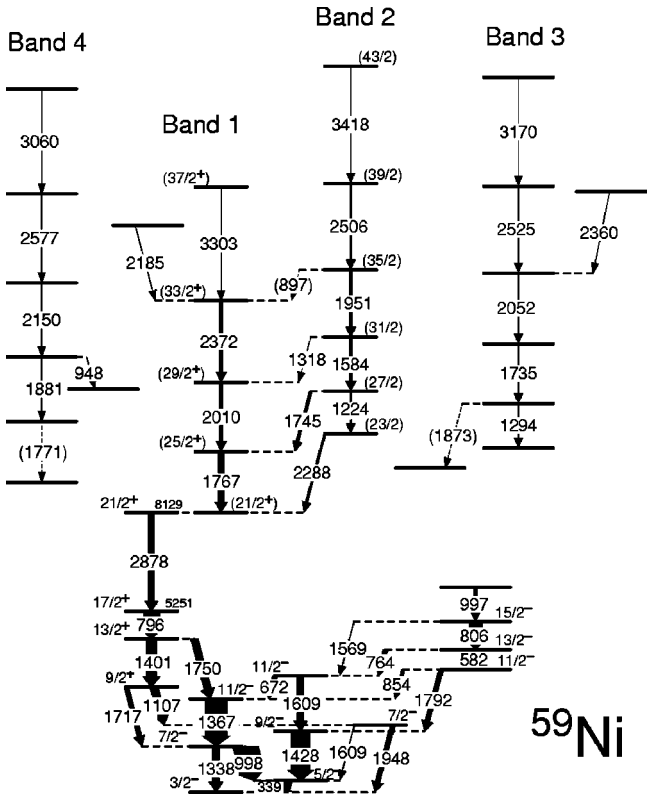

FIG. 1. Level scheme of the four highly-deformed rotational bands in ^{59}Ni established in the present study, together with selected low-spin transitions that were observed in coincidence with the rotational bands.

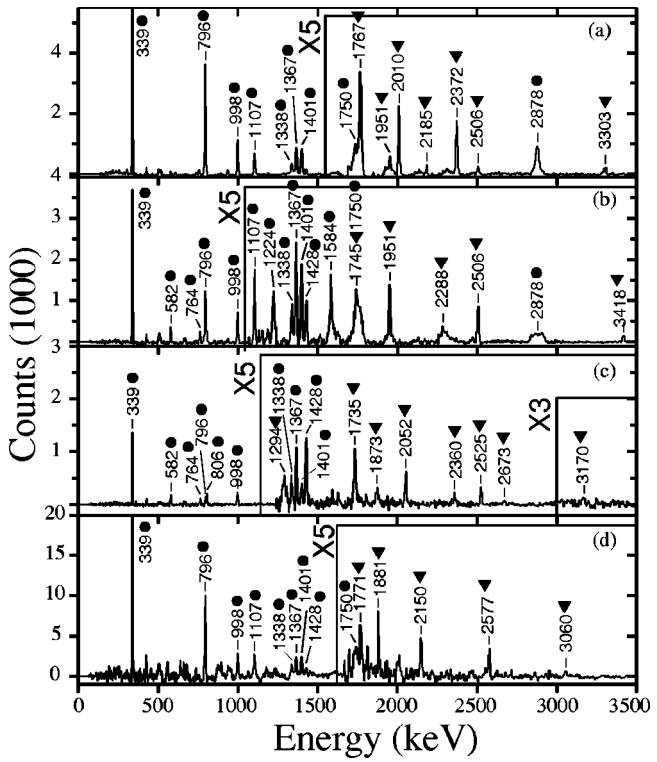

FIG. 2. (a)–(c) Coincidence spectra obtained by summing all possible double gates in bands 1–3 in ^{59}Ni, respectively. (d) Spectrum obtained by summing all clean gates in band 4. Triangles indicate members of the bands and circles indicate the low-spin ND transitions.

associated with the deformed bands were emitted at near maximum recoil velocities, when the ions were traveling in the target and backing materials, whereas the slower, low-spin decays occurred while the ions were in vacuum and traveling at a constant speed of $v/c \approx 0.027$. Because of this difference, the $\gamma\gamma\gamma$ cube has Doppler corrections performed at two recoil velocities. For $E_\gamma > 1500$ keV, we used $v_{\rm rec}/c = 0.040$, which corresponds to fast decays of deformed, rotational bands. For $E_\gamma < 1500$ keV, we used $v_{\rm rec}/c = 0.027$, which corresponds to the decays of low-spin, spherical states. As a result, spectra show narrow peaks for both fast and slow transitions with only a few exceptions. Samples of such spectra for the four deformed bands in ^{59}Ni are shown in Figs. 2(a)–(d).

In order to extract information on γ-ray multipolarities, data were summed up from the 30 most forward and backward detectors (at 17.3°, 31.7°, 37.4°, 142.6°, 148.3°, and 162.7°), and the 30 detectors near 90° (at 79.2°, 80.7°, 90°, 99.3°, and 100.8°) to form two groups labeled as ''30°'' and ''83°,'' respectively. (The labels represent the effective angles corresponding to the averaged cosines of the two detector groups.) For each band, a 30°-versus-all and an 83°-versus-all matrix were created while requiring a third γ ray being a transition in this band (detected at any angle). From these matrices, information of averaged triple directional correlations (ATDC) was obtained by extracting ratios defined as

$$\frac{I(30°)}{I(83°)}(\gamma_1) = \frac{I(\gamma_1 \text{ at } 30°, \text{ gated on } \gamma_2, \gamma_3 \text{ at any } \theta)}{I(\gamma_1 \text{ at } 83°, \text{ gated on } \gamma_2, \gamma_3 \text{ at any } \theta)}.$$

Figure 3(a) shows these ATDC ratios for clean, strong transitions in bands 1–4, as well as for some ND dipole (squares) and quadrupole (open circles) transitions at low

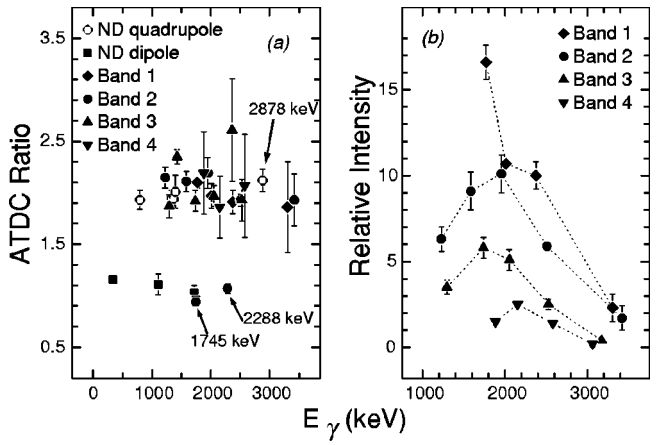

FIG. 3. (a) Averaged triple directional correlation (ATDC) ratios measured for clean, strong transitions in bands 1–4, compared to those of the known [7] $E2$ (open circles) and dipole (squares) ND transitions at low spins. (b) Intensities of the four bands in ^{59}Ni measured relative to that of the 339-keV ND transition ($\equiv 100$) at low spin.

spin. For all the measurable in-band transitions, their ATDC ratios show stretched-quadrupole characteristics. This agrees with the assumption that the observed four bands are cascades of $E2$ transitions.

Among the four established bands, band 1 is the most strongly populated, see Fig. 3(b). The spectrum obtained by summing all possible double gates in this band is shown in Fig. 2(a), and it shows that it is in coincidence with the low-spin ND transitions in ^{59}Ni. The previous study [7] of ^{59}Ni had established the highest positive-parity state to be the $17/2^+$ level at 5251 keV. Our study firmly added the 2878-keV transition on top of this level. Measured ATDC ratio shows that the 2878-keV transition has a stretched quadrupole character. Therefore, the spin and parity of the 8129-keV level were determined to be $21/2^+$. Coincidence spectra indicate that bands 1 and 2 decay to low-spin ND states through the 2878- and 796-keV transitions. Intensity and coincidence relationships also suggest that the final level of the 1767-keV transition in band 1 is most likely the same as the $21/2^+$ level at 8129 keV. However, there is a small possibility that unobserved weak, multipath connecting transitions may exist between band 1 and the 8129-keV level. Because of this uncertainty, the spins and parity of band 1 are placed in parentheses in Fig. 1.

Band 2 is only slightly weaker than band 1. A coincidence spectrum obtained by summing all combinations of double gates in band 2 is shown in Fig. 2(b). A major portion of this band decays into the initial state of the 1767-keV transition in band 1 through the 1745-keV transition. Most of the remaining intensity then decays into the final state of the 1767-keV transition via a 2288-keV γ ray. ATDC ratios show that both 1745- and 2288-keV transitions have dipole characteristics. The spins of band 2 are, therefore, assigned based on this as well as the spins assigned to band 1. In addition to strong connections to the positive-parity, 2878-, 796-keV low-spin branch, band 2 is also weakly in coincidence with the low-spin 806- and 582-keV ND transitions. Connecting transitions to this branch, however, could not be established.

Bands 3 and 4 are weaker than bands 1 and 2. Although no connecting transitions could be established between bands 3 and 4 and the low-spin ND states in ^{59}Ni, the clean and strong coincidences between these two bands and the low-spin ND states leave very little doubt that they belong to ^{59}Ni. Figures 2(c) and (d) illustrate such coincidences. ATDC ratios measured for bands 3 and 4 show that transitions in these bands are stretched quadrupole transitions. Spins and parities of these two bands, however, could not be established.

To estimate the deformation associated with the deformed bands, the centroid-shift Doppler attenuation method [8,9] was used to measure the averaged transition quadrupole moments, Q_t, for the more intensely populated bands 1 and 2. Using the technique described in Refs. [8,9], the relative velocity of the recoils, $F_\tau = v(E_\gamma)/v_{\max}$, were extracted and shown in Fig. 4(a) together with calculations. [$v(E_\gamma)$ is the average recoil velocity at the time when E_γ is emitted, and $v_{\max}$ is the maximum recoil velocity for the $2\alpha 2p$ reaction channel.] The calculated curves were produced by the LINESHAPE program [10] and used the stopping powers in Ref.

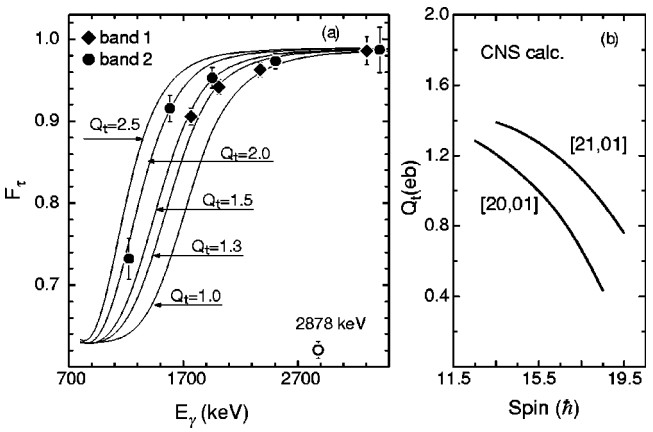

FIG. 4. (a) Experimental (filled symbols) and calculated (curves) values of F_τ as a function of E_γ for band 1 and band 2. (b) Q_t values obtained from CNS calculations for the [20,01] and [21,01] ($\alpha = -1/2$) configurations assigned to bands 1 and 2, respectively.

[11] (corrected according to Ref. [12]). The simulations used a time step of 0.7 fs and produced 5000 histories. Side feedings were modeled by a two-level rotational sequence into each state with the same Q_t and $J^{(2)}$ values as the band. Uncertainties associated with these assumptions and those with stopping powers are not included in the final results, but are expected to be smaller than the shown errors. Additional errors include a possible uncertainty in the average initial recoil velocity used for simulating the F_τ curves. Because the Microball has a larger α-particle detection efficiency at forward angles, the recorded data may have an average initial recoil velocity that is smaller than if the Microball's efficiency were isotropic, as assumed during the simulation. Although this systematic error could not be accurately corrected for the present data set, it is estimated to be smaller than the error bars shown in Fig. 4(a).

Figure 4(a) shows that when comparing the experimental data to simulated F_τ curves, it is difficult to extract a single Q_t value for each band, especially for band 2. In other words, the deformation of these two bands changes gradually as a function of spin. For band 1, the Q_t decreases from ~ 1.5 eb to ~ 1.1 eb. For band 2, the decrease is more dramatic, ranging from $Q_t \sim 2.0$ to ~ 1.1 eb. More discussions on the decrease of deformation in bands 1 and 2 are presented in ensuing paragraphs.

Lifetimes could not be extracted for bands 3 and 4 due to their weak intensities. However, data show that transitions in these two bands have a similar time scale as those of bands 1 and 2. In other words, they are much faster transitions than the low-spin ND transitions.

To understand the observed four rotational bands in ^{59}Ni, configuration-dependent cranked Nilsson-Strutinsky (CNS) calculations [13] were carried out and compared to experimental data. These calculations do not include pairing. Therefore, they are realistic at high spins, but also give qualitative descriptions for lower-spin states. The ground state of ^{59}Ni can be viewed as the ^{56}Ni core plus three valence neutrons occupying the $f_{5/2}p_{3/2}$ orbitals. Deformed, higher-spin configurations are formed by making particle excitations into

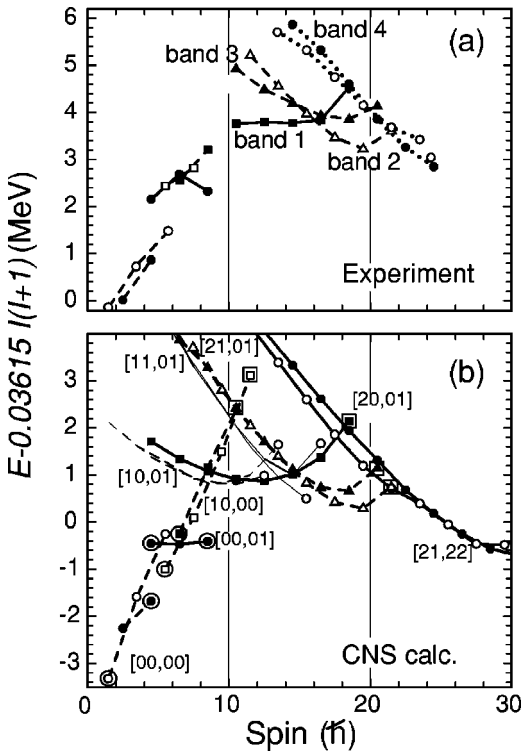

FIG. 5. Energies [relative to a liquid-drop expression $0.03615I(I+1)$] for observed (upper panel) and calculated (lower panel) bands in ^{59}Ni. Positive- and negative parities are drawn in full and dashed lines, respectively. Closed and open symbols represent $\alpha=1/2$ and $-1/2$ states, respectively. The observed band 4 is drawn with two alternative spin assignments. Calculated aligned states are indicated by large open circles and states which remain collective at $I=I_{max}$ by large open squares. The calculated bands with no experimental data are drawn with thin lines. The absolute normalization between the observed and calculated states is arbitrary.

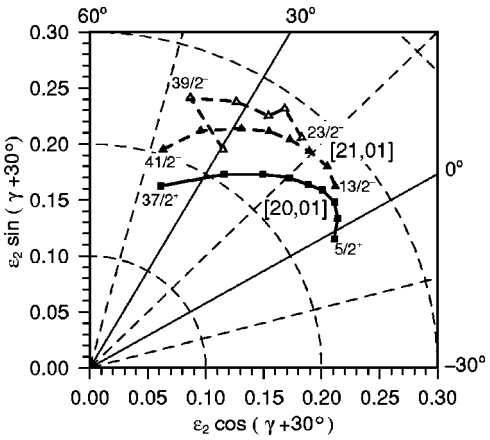

FIG. 6. Calculated shape trajectories for the [20,01] (squares) and [21,01] (open and closed triangles) configurations assigned to the observed bands 1 to 3.

the deformation-driving $g_{9/2}$ orbitals and generating holes in the $f_{7/2}$ orbitals. In the following discussion, configurations are labeled as $[p1p2,n1n2]$, which denotes $p1$ ($n1$) number of $f_{7/2}$ proton (neutron) holes and $p2$ ($n2$) number of $g_{9/2}$ proton (neutron) particles. Thus the ground state in ^{59}Ni has the [00,00] configuration.

For spin values of $I=21/2$ to $29/2\hbar$, CNS calculations show that the yrast or near yrast high-spin configuration is [20,01]. This corresponds to two proton holes generated in the $f_{7/2}$ orbitals and one neutron excited from the $f_{5/2}p_{3/2}$ states to the deformation-driving $g_{9/2}$ orbital. Such a configuration is the best candidate for the observed deformed band 1. Figure 5 shows that the calculated energy pattern for this configuration agrees with that of the observed band 1 reasonably well.

At higher spins ($I=29/2$ to $37/2\hbar$), the [21,01] configuration becomes yrast. This corresponds to two proton holes in the $f_{7/2}$ orbitals, plus one proton and one neutron excited to the deformation-driving $g_{9/2}$ orbitals. The experimentally observed bands 2 and 3 are the most likely candidates for the two signatures of this configuration. Calculated energy patterns for this configuration qualitatively describe the experimental energies of bands 2 and 3, see Fig. 5 (for this figure, the experimental band head of band 3 was assumed to be 9.3 MeV). Based on this assignment, both bands 2 and 3 will have negative parity, and the 1745- and 2288-keV connecting transition would be $E1$ transitions, which is consistent with their experimentally measured dipole characteristics.

For bands 1 to 3, the most interesting feature is their change of collectivity as a function of spin. This is partially reflected in the energy plot shown in Fig. 5(a), where all three bands show a smooth upbend towards the observed highest spins. Such a phenomenon has been observed in, e.g., ^{64}Zn [1] and ^{62}Zn [2], and has been interpreted in terms of ''smoothly-terminating bands.'' Such bands are collective at low spins but gradually become less collective and terminate in a noncollective particle-hole (terminating) state at the maximal spin. In the case of ^{59}Ni, CNS calculations of shape trajectories (Fig. 6) show that the [20,01] (assigned to band 1) and both signatures of the [21,01] (assigned to bands 2 and 3) configurations are triaxial, with quadrupole deformation ϵ_2 decreasing and γ increasing as a function of spin. This results in a decreasing Q_t, as observed in the experiment. Measured Q_t's shown in Fig. 4(a) agree with this trend for both bands 1 and 2. For comparison, Q_t's for the [20,01] and [21,01] ($\alpha=-1/2$) configurations assigned to bands 1 and 2 obtained from the CNS calculations (based on the microscopic density distribution described in Ref. [14]) are shown in Fig. 4(b). The calculated Q_t's qualitatively reproduce the experimental results of a larger average Q_t for band 2 than for band 1. Quantitatively, however, calculated Q_t's are smaller than experimental values, especially for band 2.

The [20,01] configuration assigned to band 1 has the $\pi(f_{7/2})_6^{-2}(p_{3/2}f_{5/2})_4^2 \otimes \nu(p_{3/2}f_{5/2})_4^2(g_{9/2})_{4.5}^1$ structure (superscriptions denote particle or hole numbers, and subscriptions denote corresponding maximum spins in various subshells). Thus the maximal spin for band 1 is $I_{max}=6+4+4+4.5=37/2^+$. Similarly, the [21,01] ($\alpha=-1/2$) configuration assigned to band 2 has the $\pi(f_{7/2})_6^{-2}(p_{3/2}f_{5/2})_{2.5}^1(g_{9/2})_{4.5}^1 \otimes \nu(p_{3/2}f_{5/2})_4^2(g_{9/2})_{4.5}^1$ structure and results in a maximal spin of $I_{max}=6+2.5+4.5+4+4.5=43/2^-$. Experimentally, the tentatively assigned spins for these bands indicate that these

I_{max} states have been observed. Calculations also show that at $I=I_{max}$, these bands are triaxial with $\gamma\sim45°$, instead of reaching the noncollective oblate shape of $\gamma=60°$. Therefore, substantial collectivity remains even for these $I=I_{max}$ states. In most previous experimental studies of terminating properties of rotational bands, the states at $I=I_{max}$ were understood as corresponding to the nuclear angular momenta being fully aligned along the symmetry axis of a noncollective oblate shape ($\gamma=60°$). In ^{59}Ni the bands are reminiscent of rotational bands at large deformation in a pure oscillator, which never terminate because of strong couplings between the N shells [15,16]. In a similar manner, the coupling between the $f_{7/2}$ subshell and other $N=3$ subshells in ^{59}Ni causes these bands to be partially collective at the $I=I_{max}$ states. Because of these couplings, it is possible to build $I=I_{max}$ states at a lower energy cost with additional small spin contributions from the core, before the spin vectors from *active* particles are fully aligned. In ^{59}Ni, e.g., the $f_{7/2}$ neutron subshell is fully occupied by eight neutrons, but it gives a small yet important contribution to the total spin at the $I=I_{max}$ state. The above features have been previously discussed in the $A=80$ region [17], although corresponding rotational bands have not been observed experimentally to their $I=I_{max}$ states. Our study of ^{59}Ni represents one of the first two experimental cases where these partially collective $I=I_{max}$ states have been identified. (Similar effects have recently been observed [18] in ^{59}Cu.)

The configuration assignment for band 4 is more uncertain. A possible candidate is the [21,22] configuration, which corresponds to an additional neutron excited to the $g_{9/2}$ orbital and two neutron holes generated in the $f_{7/2}$ orbital compared to bands 2 and 3. Such a configuration has a significantly larger deformation and it does not terminate. Figure 5 shows that based on this assignment, the calculated energies give the best fit to the experimentally observed energies of band 4, assuming that the observed states are given the spin range of $I=27/2-47/2$ with a band head energy of 13.8 MeV [open circles in Fig. 5(a)], or $I=29/2-49/2$ with a band head energy of 15 MeV [closed circles in Fig. 5(a)].

To summarize, four highly-deformed rotational bands were established in ^{59}Ni. Based on CNS calculations, three of the four bands were interpreted as reaching their maximal-spin states with active particles distributed over the $f_{7/2}$, $(p_{3/2},f_{5/2})$ and $g_{9/2}$ subshells. Unlike most bands of this type observed previously, calculations indicate that these bands in ^{59}Ni have substantial collectivity at the $I=I_{max}$ states. Such a phenomenon represents one of the first cases where partially *collective* maximal-spin states have been observed.

Oak Ridge National Laboratory is managed by UT-Battelle, LLC, for the U.S. DOE under Contract No. DE-AC05-00OR22725. This work was also supported by the U.S. DOE [Contract Nos. DE-AC05-76OR00033(ORISE) and DE-FG05-88ER40406(WU)], the Natural Science and Engineering Research Council of Canada, the German BMBF (Contract No. 06Ok958), and the Swedish Research Council.

[1] A. Galindo-Uribarri *et al.*, Phys. Lett. B **422**, 45 (1998).
[2] C.E. Svensson *et al.*, Phys. Rev. Lett. **80**, 2558 (1998).
[3] I. Ragnarsson *et al.*, Phys. Scr. **34**, 651 (1986), and references therein.
[4] V.P. Janzen *et al.*, Phys. Rev. Lett. **72**, 1160 (1994).
[5] I.Y. Lee, Nucl. Phys. **A520**, 641c (1990).
[6] D.G. Sarantites *et al.*, Nucl. Instrum. Methods Phys. Res. A **381**, 418 (1996).
[7] S. Juutinen *et al.*, Nucl. Phys. **A504**, 205 (1989).
[8] B. Cederwall *et al.*, Nucl. Instrum. Methods Phys. Res. A **354**, 591 (1995).
[9] C.-H. Yu *et al.*, Phys. Rev. C **57**, 113 (1998).
[10] J. C. Wells *et al.*, LINESHAPE: A Computer Program for Doppler Broadened Lineshape Analysis, ORNL Physics Division Prog. Rep. 30, 1991, No. ORNL-6689.
[11] L.C. Northcliffe and R.F. Schilling, Nucl. Data Tables **7**, 233 (1970).
[12] J.F. Ziegler and W.K. Chu, At. Data Nucl. Data Tables **13**, 463 (1974).
[13] T. Bengtsson and I. Ragnarsson, Nucl. Phys. **A436**, 14 (1985); A.V. Afanasjev and I. Ragnarsson, *ibid.* **A591**, 387 (1995).
[14] A. Juodagalvis, I. Ragnarsson, and S. Åberg, Phys. Lett. B **477**, 66 (2000).
[15] T. Troudet and R. Arvieu, Z. Phys. A **291**, 183 (1979).
[16] I. Ragnarsson, Phys. Lett. B **199**, 317 (1987).
[17] A.V. Afanasjev, B.D. Fossan, G.J. Lane, and I. Ragnarsson, Phys. Rep. **322**, 1 (1999).
[18] C. Andreoiu *et al.* (to be published).